ICPS5

Behavior of Concrete Reinforced with Fibers from End-of-Life Tires Under High Compressive Strain Rates

Małgorzata PAJĄK[1]*, Jacek JANISZEWSKI[2], Leopold KRUSZKA[2]

[1] *Department of Structural Engineering*
Silesian University of Technology
Akademicka 2A, 44-100 Gliwice, Poland
*Corresponding Author e-mail: malgorzata.pajak@polsl.pl

[2] *Military University of Technology*
Urbanowicza 2, 00-908 Warsaw, Poland
e-mail: jacek.janiszewski@wat.edu.pl

The behavior of concrete reinforced with the fibers obtained from the end-of-life tires under high compressive strain rates was the scope of this research. The laboratory investigations were performed using the Hopkinson Pressure Bar with a diameter of 40 mm. The waste fibers with untypical geometrical parameters were applied to concrete with a dosage of 30 kg/m^3. The pronounced increase of compressive strength of the RSFRC, when subjected to high strain rates, was observed. The strain rate sensitivity of the RSFRC expressed by DIF was comparable to the other results presented in the literature.

Key words: Hopkinson bar; fiber reinforced concrete; fibers from end-of-life tires; high compressive strain rates.

1. Introduction

Cement-based materials reinforced with randomly distributed fibers are commonly used in concrete defense structures, civil infrastructure (bridges, tunnels, rockfall protection galleries), building structures in the energy sector (water tanks, nuclear containment vessels) or civil buildings (industrial floors). These structures currently must withstand natural hazards such as tornadoes, ocean waves or earthquakes [1, 2]. The man-made accidents or terrorist-induced projectile impact or explosions should also be considered [3, 4].

Nowadays, the manufactured fibers are mainly used as a reinforcement of concrete. The present paper deals with fibers coming from the end-of-life tires.

Considering the problem of the disposal of used tires, every opportunity to re-use tire components is valuable. One of the components created in the recycling process is a steel cord. The geometrical characteristic of the recycled steel fibers (RSF) differs much from typical fibers. The length of the fibers depends on the process of their reclamation, and because they are an integral part of the tire, it is impossible to obtain the fibers of one length. Thus, as a result, the fibers with a small diameter and various lengths are obtained. It is also not possible to avoid some rubber particles in the mix. As a result of all these features, RSF are not frequently applied in structural elements, even though the investigation of concrete reinforced with RSF under static conditions does not show obstacles in the application of waste fibers to concrete [5, 6].

Furthermore, the RSF can be a substitute for short, straight fibers of a very small diameter used as a component in many new types of ultra-high perfor-mance fiber reinforced concrete (UHPFRC) investigated by many researchers [3, 7–14]. The high amount of the fibers is added to concrete, what signifi-cantly increases the costs of those types of concrete [13]. In the case of ap-plication of RSF, not only the economic but also environmental benefits can be achieved.

Generally, the fibers have a minor effect on the same value of the compressive strength under static conditions. The pronounced influence of fibers is noted on post-peak parameters of concrete. The fibers delay the appearance of the micro-cracks and bridge the macro-cracks. Under static conditions, the micro-cracks slowly propagate into macro-cracks [2]. In case of dynamic loading, the time of fracture of concrete is very short. At once, micro-cracks develop into macro-cracks, and other micro-cracks appear. As a result, more energy is consumed and the higher value of compressive strength is observed [1, 3, 4, 7–13, 15–21]. Considering fibers, more of them participate in a fracture process under dynamic than static conditions. Thus, their effect is more pronounced under dynamic than under static loading. As a result, the strain rate sensitivity of concrete reinforced with fibers based on the Hopkinson Bar tests is lower than the plain matrix under compression [16–18] and tension [19]. However, some researches indicate that under shear loading the influence of fibers is limited [20].

This paper discusses the preliminary results of an ongoing experimental pro-gram carried out with the use of the Split Hopkinson Pressure Bar to investigate the effect of RSF on strain rate sensitivity of concrete. The concrete reinforced with different types of fibers [7–13, 17] and composites [21] was studied with the use of SHPB. However, the RSF has never been investigated in the existing literature.

In this study, the complete dynamic stress-strain curves are analyzed and discussed. The main results are presented using the state-of-the-art technology and methods.

2. Experimental investigation

2.1. Materials

The concrete reinforced with fibers coming from the end-of-life tires (RSFRC) is the scope of this study interest. The detailed composition of a matrix is presented in Table 1. The Portland cement CEM I 32.5R, locally available sand, coarse aggregate, and silica fume were used to create the concrete matrix. The silica fume was used in the amount of cement equal to 10%. The water to binder (cement with silica fume) ratio was equal to 0.58.

Table 1. The composition of the RSFRC.

Cement CEM I 32.5R [kg/m^3]	Natural sand (0–2 mm) [kg/m^3]	Coarse aggregate (2–16 mm) [kg/m^3]	Silica fume [kg/m^3]	Water [kg/m^3]	Steel fibers (%) by volume	W/B
350	622	1036	33	221	0.38	0.58

The general view of the recycled steel fibers is presented in Fig. 1 and their parameters are summarized in Table 2. In Fig. 1 it can be seen how different from typical fibers the longitudinal shape of RSF was. The stochastic length of RSF which was in a range of about 2–30 mm is clearly visible. Among the fibers, some rubber particles and also a few fibers of a bigger diameter can be found. The dosage of waste fibers was equal to 30 kg/m^3, what was adequate to the volume ratio of 0.38%.

Table 2. Properties of fibers from the end-of-life tires (RSF).

Length [mm]	Diameter [mm]	Tensile strength [MPa]	Aspect ratio (length/diameter)	Longitudinal shape
2÷30	0.15 ± 5%	≥ 2850	13÷200	irregular (curved, twisted)

Fig. 1. Fibers from end-of-life tires – recycled steel fibers (RSF).

The fibers decreased the workability of the concrete. However, no negative influence on the rheological parameters of the matrix was noticed. The fibers were distributed homogeneously in the concrete matrix during the mixing process.

The cylinders (150×300 mm) and beams with the dimensions of $100 \times 100 \times 500$ mm were prepared. The static compressive tests were performed on cylinders in the servo-hydraulic testing machine. The specimens for the dynamic tests with the diameter of 40 mm were cut from the beams, and the external surfaces were polished to ensure their parallelity. This method was chosen to ensure the homogenous distribution of fibers in the specimen tested under dynamic conditions. All the specimens were prepared at the Silesian University of Technology.

2.2. Strength tests

The RSFRC specimens were tested under static compression in 3000 kN hydraulic compression testing machine with the constant rate of loading. The compressive tests were performed on cylinder specimens with a diameter of 150 mm and height of 300 mm. Five specimens were tested in compression at the age of 28 days. The static tests were performed at the Silesian University of Technology.

The quasi-static compression strength of the concrete reinforced with waste fibers was equal to 46.4 MPa. The strength of plain concrete where no fibers were added was equal to 45.4 MPa. Thus, as in case of manufactured fibers the waste fibers insignificantly increased the fc of concrete. The research dealing with the influence of the fibers on flexural parameters of the same mix as presented in the paper can be found in [6]. Based on it, the fibers increase the post-peak flexural parameters, however slightly.

The dynamic compressive behavior of RSFRC was studied with the use of the Split Hopkinson Pressure Bar (SHPR) recently built at the Military University of Technology (Fig. 2). This testing arrangement is equipped with bars of a large diameter, what makes it suitable to test the specimens made from brittle RSFRC. The SHPB consists of the incident, transmitted and striker aluminum bars of diameter equal to 40 mm. The diameter and height of each specimen were equal to 40 mm. During the test, the specimen fell apart into many pieces which splattered at high speed in every direction. To ensure safety, it was necessary to mount the timber safety box around the RSFRC specimen (Fig. 2). The total length of the device which is equal to 12 m was determined by the diameter of the bars. The polymer wave-shapers were used to achieve the equilibrium state in the specimen. Three specimens were tested for each of two analyzed impact velocities. The specimens were tested under dynamic conditions at the age of 60–90 days.
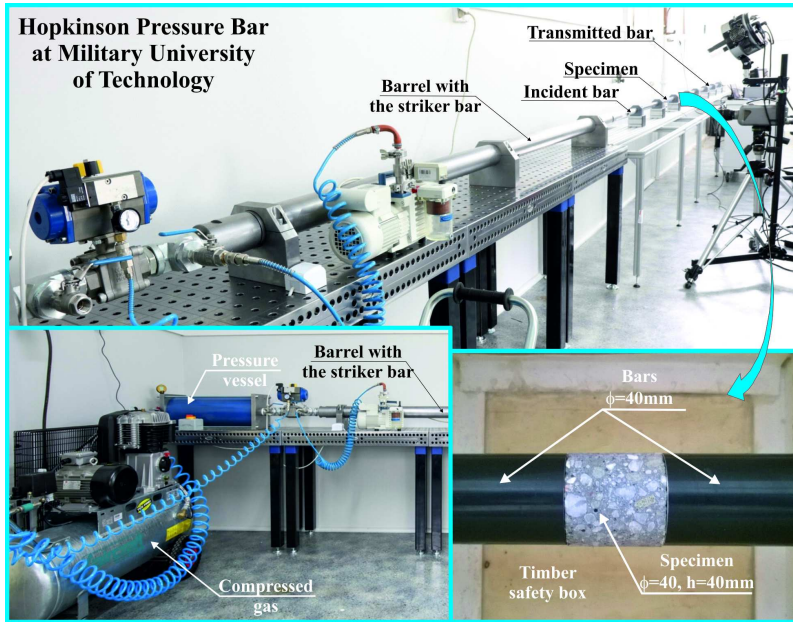
FIG. 2. The Hopkinson Pressure Bar with RSFRC specimen sandwich between the Hopkinson bars.

3. RESULTS AND DISCUSSION

3.1. Wave profiles in the bars

The propagation of the waves in the bars during the tests performed with two impact velocities is presented in Fig. 3. It can be noted that the plateau of the
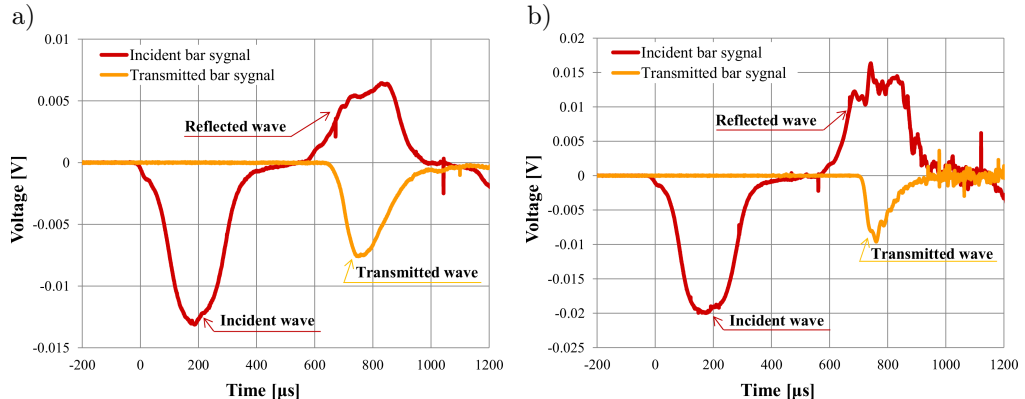

FIG. 3. The signals in the incident bar and transmitted bar obtained in the tests with: a) lower impact velocity and b) higher impact velocity.

reflected wave was reached in the time corresponding to the maximum value of the transmitted wave, what is desired considering the SHPB test requirements.

During the Hopkinson Pressure Bar test, the striker bar impacts on the incident bar and produces the compressive strain wave (ε_i). The wave propagates through the incident bar to be divided into transmitted (ε_t) and reflected part (ε_r) when reaching the interfacial surface of the specimen. The wave propagation is measured at the center of each bar with the use of a pair of strain gages attached symmetrically onto the opposite surfaces of the bars.

Assuming that the specimen is in the equilibrium state, the stress and strain in the specimen and strain rate can be calculated based on Eqs (3.1)–(3.3). The specimen strain can be determined directly from reflected wave using Eq. (3.1). The transmitted wave is proportional to the specimen strength and can be used for its calculation based on Eq. (3.2), while the reflected wave is used for strain rate calculation (3.3)

$$(3.1) \qquad \varepsilon_h(t) \;=\; \frac{2c_A}{L} \int\limits_0^t \varepsilon_r(t)\,\mathrm{d}t,$$

$$(3.2) \qquad \sigma_h(t) \;=\; \frac{A_A E_A}{A_P}\varepsilon_t(t),$$

$$(3.3) \qquad \dot{\varepsilon}_h(t) \;=\; \frac{2c_A}{L}\varepsilon_r(t),$$

where L, A_P are the length and the cross-sectional area of the specimen, and E_A, A_A, c_A are the Young's modulus, the cross-sectional area and the elastic wave velocity of the pressure bar, respectively.

3.2. Stress-strain diagrams

The compressive strength of RSFRC under static conditions was equal to 46.4 MPa. The RSFRC specimens were tested using two impact velocities, what produced the strain rates of 83 to 152 s^{-1} in the specimens. The stress-strain curves obtained in the tests performed with two impact velocities are graphically presented in Fig. 4. The main results from the dynamic tests of RSFRC are presented in Table 3.

The strain rate effect was observed for RSFRC. The increase of strength with the increase of strain rate was noted. Meanwhile, the strain at peak strength and toughness decreased with the increase of strain rate. For lower impact velocity, the strain rates were in a range of 83–98 s^{-1}. The plottings of the strain-stress curves are comparable, what can be seen in Fig. 4. In the case of higher impact velocities, the strain rates were equal to 142 and 152 s^{-1}. The scattered plotting was more pronounced in the case of higher strain rates (matched with
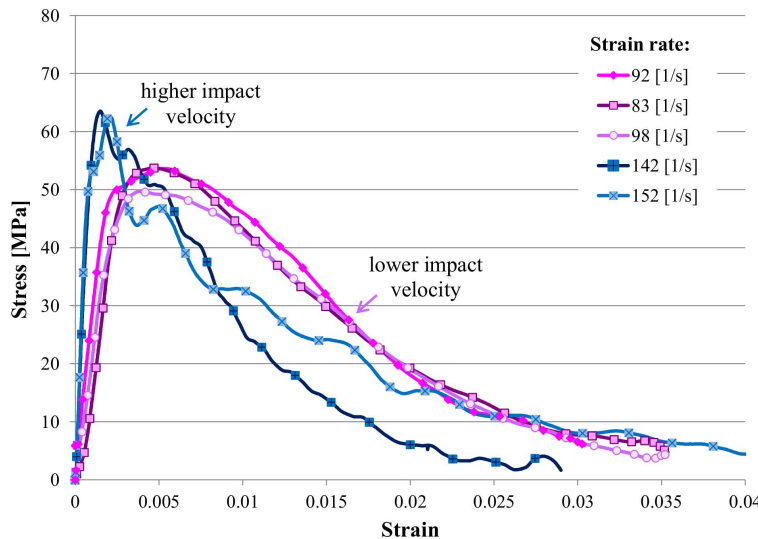
Fɪɢ. 4. Stress-strain diagrams obtained in the Hopkinson Pressure Bar tests on RSFRC.

Table 3. Main results from tests of RSFRC under high strain rates.

Strain rate [1/s]	Static compressive strength [MPa]	Dynamic compressive strength [MPa]	DIF	Average DIF	Strain at peak stress $\times 10^{-3}$	Toughness [Nm]
92		53.62	1.16		2.32	91.4
83		53.70	1.16	1.12	4.70	87.9
98	46.4	49.68	1.07		5.41	85.8
142		63.52	1.37	1.36	0.82	63.2
152		62.63	1.35		0.75	80.2

blue in Fig. 4). This can be attributed to the fact that in the case of higher strain rates the equilibrium state was less satisfied. Moreover, this led to conclusion about the modification of the device to achieve the equilibrium state in the specimen for the higher impact velocities.

The determination of strain rate in HPB tests is crucial for comparison purpose. In Fig. 5 the variation of strain rate, stress in the specimen and the method of determination of strain rate are shown. The preliminary tests were conducted to choose the suitable wave-shaper considering the equilibrium state. The example of the equilibrium state obtained in the test with lower impact velocity is presented in Fig. 6. In the present paper, the strain rate was assigned as an average during almost the entire process of loading. The average strain rate was calculated from the strain rate corresponding to 30% of the maximum stress un-
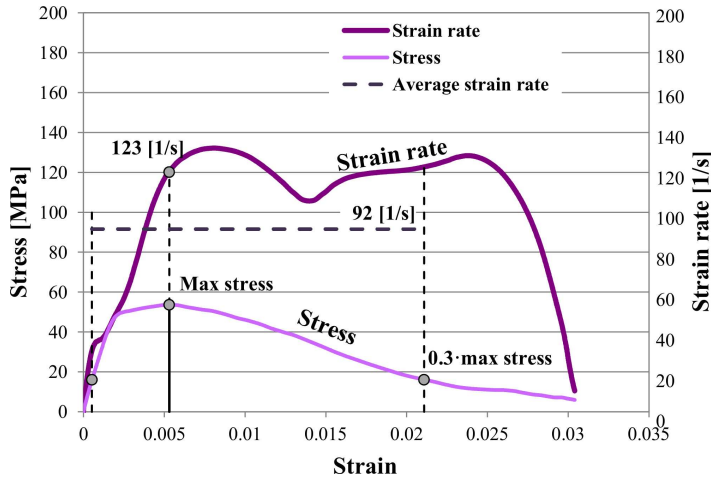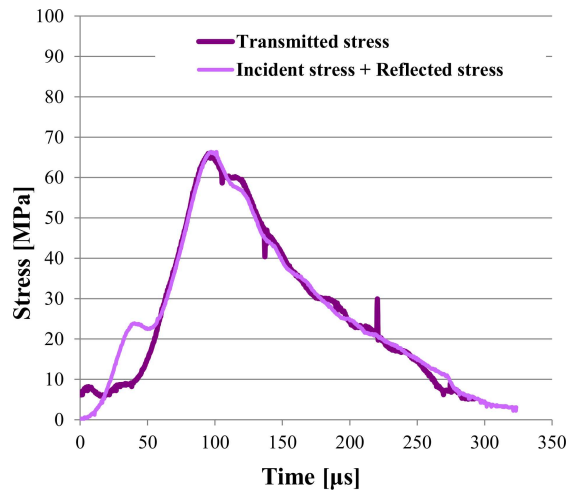
Fig. 5. The determination of strain rate.

Fig. 6. The equilibrium state in the specimen tested with lower impact velocity.

til the same point after the failure. In some papers, the strain rate at maximum stress was presented. In other works, the average strain rate was calculated from the values of the strain rate at a plateau, what in the authors' opinion is the most appropriate approach. It is desired to achieve the plateau in the strain rate in the post-elastic phase. In the present investigation, this condition was difficult to fulfill. It is worth to point out that other researchers also indicated the problem of achieving the constant strain rate [17]. However, our research allows to draw conclusions for further research. Based on our experiments the conclusions were

made about the shape of the striker that should be used to achieve the desired variation of strain rate.

3.3. Dynamic Increase Factor

The influence of various types of industrial fibers on the mechanical parameters of cement-based materials under high strain rates was analyzed in details in [22]. In the literature, different types of concrete reinforced mainly with a high volume ratio of fibers reaching 4% were tested. It was observed that the strain rate sensitivity of cement-based materials decreases with the addition of fibers. In other words, the dynamic compressive strength of fiber reinforced concrete is lower than that of plain concrete. This relationship is dependent not only on the amount and shape of fibers but also on the properties of the matrix [22].

In Fig. 7, the comparison of dynamic increase factor (DIF) obtained in the latest investigations discussed in [7–13, 17] is depicted. The description presented in Fig. 7 contains the author(s) name, year of publication and the fibers volume content that was applied to the matrix. The DIF is the ratio of dynamic compressive strength to static compressive strength. The average values of DIF obtained in the present research were equal to 1.12 and 1.36 for two investigated impact
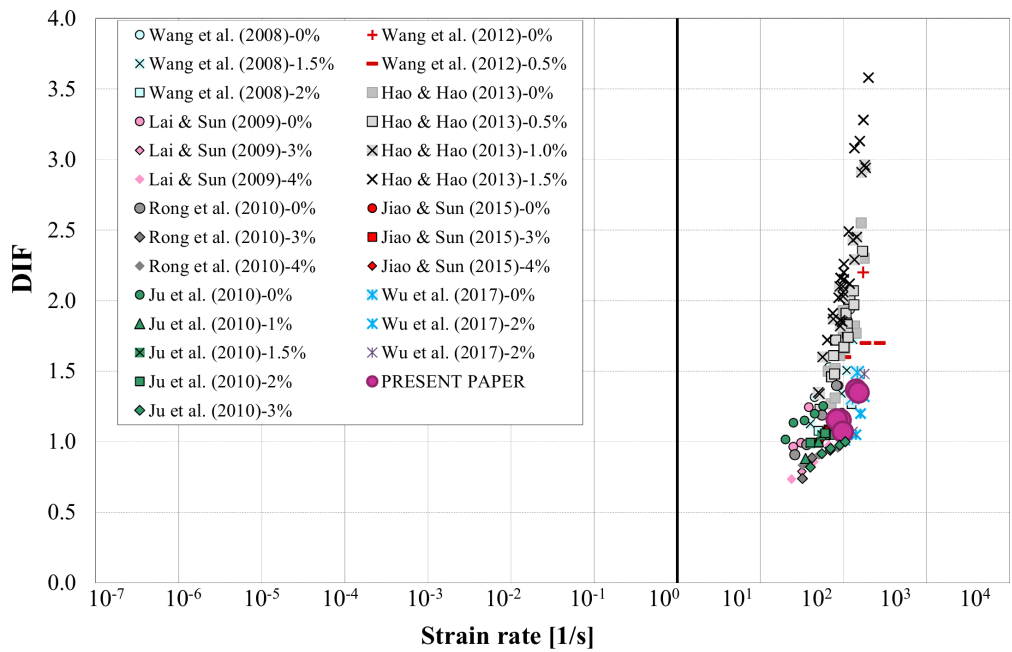

FIG. 7. Strain rate sensitivity of cement-based materials reinforced with fibers.

velocities, respectively (Table 3). These results of the preliminary research are comparable to the results obtained by other researchers, what can be seen in Fig. 7.

The dynamic compressive strength in almost all research did not exceed twice the static compressive strength. Furthermore, the strain rate sensitivity of the specimens reinforced with fibers was lower or close to the sensitivity of the matrix. The compressive strengths of those tested cement-based materials were in a range of 86–158 MPa [7–13].

The exception was the investigation performed by HAO & HAO [17], where the concrete reinforced with fibers was more strain rate sensitive than the plain matrix. In this case, the values of DIF reached the highest observed values equal to 3.6. The observed high strain rate sensitivity can be partially explained by the low compressive strength of the tested specimens, which was equal to 35.5 MPa. However, under high strain rates, the compressive strength does not seem to influence the behavior of concrete [23].

3.4. Failure pattern

As expected, the most pronounced effect of steel fibers was noted on the failure pattern. Analyzing the degree of visible destruction of the RSFRC specimens it can be observed that it increased with the impact velocity (Fig. 8). However, this difference is not pronounced. This might be attributed to the fact that only 30 kg/m^3 of RSF were added to concrete. The geometrical parameters of the fibers could also be relevant. The fibers seemed to be pulled out from the pieces of concrete. Considering the various lengths of the RSF, it is hard to draw a conclusion about breaking of any of the fibers. The characteristic cone shape in the static compression tests could be seen in case of both impact velocities.
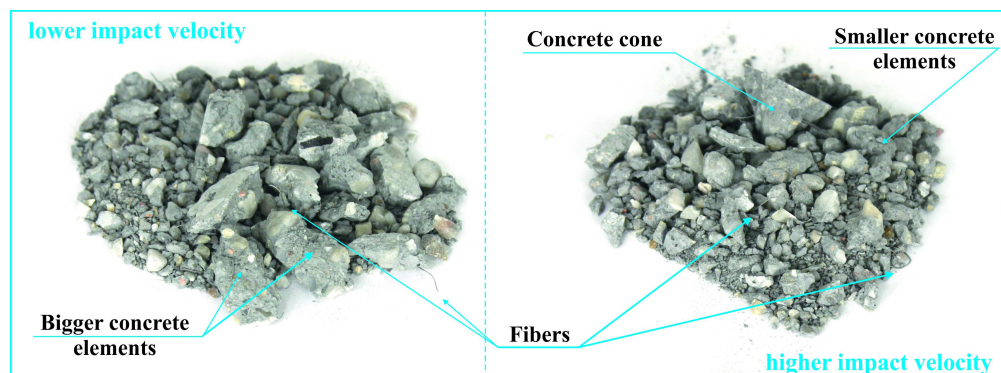

FIG. 8. RSFRC specimens after the tests with the use of SHPB.

4. Conclusions

This paper presents the results from the preliminary tests of an ongoing experimental program carried out in Poland with the use of recently built Split Hopkinson Pressure Bar of a diameter of 40 mm. The effect of the waste fibers on the behavior of concrete under the dynamic loading was investigated. The strain rate sensitivity of concrete reinforced with 30 kg/m^3 of fibers coming from the end-of-life tires (RSFRC) was confirmed. The obtained values of DIF fit well in the range of the results specified by other scientists dealing with industrial fibers. The influence of the fibers on the failure pattern was insignificant, what may be connected with the application of a comparably small amount of fibers and their geometrical characteristic.

This preliminary research indicates that the waste fibers could be a substitute for manufactured fibers in the structural application that could suffer from high strain rates. It is worth to mention the benefits to the environment that are connected with re-use of that kind of fibers.

The conducted research allowed to verify the research method and showed the directions of the device modification to achieve the desired variation of the strain rate.

Acknowledgement

References

1. Bragov A.M., Petrov Y.V., Karihaloo B.L., Konstantinov A.Y., Lamzin D.A., Lomunov A.K., Smirnov I.V., *Dynamic strengths and toughness of an ultra high performance fibre reinforced concrete*, Engineering Fracture Mechanics, **110**: 477–488, 2013.

2. Brandt A.M., *Fibre reinforced cement-based (FRC) composites after over 40 years of development in building and civil engineering*, Composite Structures, **86**: 3–9, 2008.

3. Sovják R., Vavŕiník T., Zatloukal J., Máca P., Mičunek T., Frydrýn M., *Resistance of slim UHPFRC targets to projectile impact using in-service bullets*, International Journal of Impact Engineering, **76**: 166–177, 2015.

4. Zanuy C., Ulzurrún G.S.D., *Rate effects of fiber-reinforced concrete specimens in impact regime*, Procedia Engineering, **193**: 501–508, 2017.

5. Groli G., Caldentey A.P., Marchetto F., Fernández F.A., *Serviceability performance of FRC columns under imposed displacements: An experimental study*, Engineering Structures, **101**: 450–464, 2015.

6. PAJĄK M., *Application of fibers from end-of-life tires as a self-compacting concrete reinforcement – an experimental study*, Architecture Civil Engineering Environment, **11**: 105–113, 2018.

7. WANG Y., WANG Z., LIANG X., AN M., *Experimental and numerical studies on dynamic compressive behavior of reactive powder concretes*, Acta Mechanica Solida Sinica, **21**(5): 420–430, 2008.

8. WANG S., ZHANG M-H., QUEK S.T., *Mechanical behavior of fiber-reinforced high-strength concrete subjected to high strain-rate compressive loading*, Construction and Building Materials, **31**: 1–11, 2012.

9. RONG Z., SUN W., ZHANG Y., *Dynamic compression behavior of ultra-high performance cement based composites*, International Journal of Impact Engineering, **37**(5): 515–520, 2010.

10. JU Y., LIU H.B., SHENG G.H., WANG H.J., *Experimental study of dynamic mechanical properties of reactive powder concrete under high-strain-rate impacts*, Science China Technological Sciences, **53**: 2435–2449, 2010.

11. LAI J., SUN W., *Dynamic behaviour and visco-elastic damage model of ultra-high performance cementitious composite*, Cement and Concrete Research, **39**: 1044–1051, 2009.

12. JIAO C., SUN W., *Impact resistance of reactive oowder concrete*, Journal of Wuhan University of Technology-Mater. Sci. Ed., **30**: 752–757, 2015.

13. WU Z., SHI C., HE W., WANG D., *Static and dynamic compressive properties of ultra-high performance concrete (UHPC) with hybrid steel fiber reinforcements*, Cement and Concrete Composites, **79**: 148–157, 2017.

14. DENISIEWICZ A., KUCZMA M., *Two-scale modelling of reactive powder concrete. Part III: Experimental tests and validation*, Engineering Transactions, **6**(1): 55–76, 2015.

15. ADAMCZYK R., ŁODYGOWSKI T., *Numerical modelling of laboratory test of plain concrete under uniaxial impact compression*, Engineering Transactions, **51**(4): 381–398, 2003.

16. KRUSZKA L., MOĆKO W., FENU. L., CADONI E., *Comparative experimental study of dynamic compressive strength of mortar with glass and basalt fibres*, EPJ Web of Conferences, **94**: 05008, 2015, doi: 10.1051/epjconf/20159405008.

17. HAO Y., HAO H., *Dynamic compressive behaviour of spiral steel fibre reinforced concrete in split Hopkinson pressure bar tests*, Construction and Building Materials, **48**: 521–532, 2013.

18. YOO D.-Y., BANTHIA N., YOON Y.-S., *Impact resistance of ultra-high performance fiber-reinforced concrete with different steel fibers*, 9th RILEM International Symposium on Fiber Reinforced Concrete – BEFIB, 2016.

19. CUROSU I., MECHTCHERINE V., FORNI D., CADONI E., *Performance of various strain-hardening cement-based composites (SHCC) subject to uniaxial impact tensile loading*, Cement and Concrete Research, **102**: 16–28, 2017.

20. FORQUIN P., LUKIC B., *Experimental techniques to characterize the mechanical behaviour of ultra-high-strength-concrete under extreme loading conditions*, [in:] *Dynamic Behavior of Materials, Volume 1: Proceedings of the 2015 Annual Conference on Experimental and Applied Mechanics, B. Song, L. Lamberson, D. Casem, J. Kimberley [Eds]*, pp. 229–237, 2016, doi: 10.1007/978-3-319-22452-7_32.

21. Massaq A., Rusinek A., Klósak M., Boulouz A., Koutti L., *Analysis of the composite material behaviour subjected to dynamic bending using the Hopkinson bar*, Engineering Transactions, **64**(1): 115–131, 2016.

22. Pajak M., *Dynamic response of SFRC under different strain rates – an overview of test results*, 7th International Conference Analytical Models and New Concepts in Concrete and Masonry Structures, 2011, Kraków.

23. Pajak M., *The influence of the strain rate on the strength of concrete taking into account the experimental techniques*, Architecture Civil Engineering Environment, **3**: 77–86, 2011.